The American Journal of Pathology, Vol. 175, No. 4, October 2009

DOI: 10.2353/ajpath.2009.081141

Vascular Biology, Atherosclerosis and Endothelium Biology

Alterations in Aortic Cellular Constituents during Thoracic Aortic Aneurysm Development

Myofibroblast-Mediated Vascular Remodeling

Jeffrey A. Jones,*† Christy Beck,* John R. Barbour,* Jouzas A. Zavadzkas,* Rupak Mukherjee,* Francis G. Spinale,*† and John S. Ikonomidis*

From the Department of Surgery, Division of Cardiothoracic Surgery Research, Medical University of South Carolina, Charleston; and the Ralph H. Johnson Veterans Affairs Medical Center,† Charleston, South Carolina*

The present study tested the hypothesis that changes in the resident endogenous cellular population accompany alterations in aortic collagen and elastin content during thoracic aortic aneurysm (TAA) development in a murine model. Descending thoracic aortas were analyzed at various time points (2, 4, 8, and 16 weeks) post-TAA induction (0.5 M $CaCl_2$, 15 minutes). Aortic tissue sections were subjected to histological staining and morphometric analysis for collagen and elastin, as well as immunostaining for cell-type-specific markers to quantify fibroblasts, myofibroblasts, and smooth-muscle cells. Results were compared with reference control mice processed in the same fashion. Aortic dilatation was accompanied by changes in the elastic architecture that included: a decreased number of elastic lamellae (from 6 to 4); altered area fraction of elastin (elevated at 4 weeks and decreased at 16 weeks); and a decreased area between elastic lamellae (minimum reached at 4 weeks). Total collagen content did not change over time. Increased immunoreactivity for fibroblast and myofibroblast markers was observed at 8- and 16-week post-TAA-induction, whereas immunoreactivity for smooth-muscle cell markers peaked at 4 weeks and returned to baseline by 16 weeks. Therefore, this study demonstrated that changes in aortic elastin content were accompanied by the emergence of a subset of fibroblast-derived myofibroblasts whose altered phenotype may play a significant role in TAA development through the enhancement of extracellular matrix proteolysis. ***(Am J Pathol 2009, 175:1746–1756; DOI: 10.2353/ajpath.2009.081141)***

Thoracic aortic aneurysms (TAA) develops as a result of a complex series of events that dynamically alter the structure and composition of the aortic vascular extracellular matrix (ECM).[1,2] This process is thought to be the consequence of a dysregulated balance between matrix degradation and matrix deposition, mediated primarily through the altered expression and abundance of the matrix metalloproteinases and their endogenous inhibitors.[3,4] Although it has become clear that these pathological alterations are associated with enhanced dilatation, dissection, and rupture, little is known about the events that regulate the remodeling process during TAA development.

The thoracic aorta is composed of a trilaminar wall encompassing the structural and cellular components that coordinately function to maintain aortic compliance and resiliency.[5,6] Each of the three layers carries out a primary function regulated by its endogenous constituents.[7] The innermost layer, the *tunica intima*, forms the luminal interface of the aorta and is composed of endothelial cells resting on a basement membrane. This layer regulates diffusion and migration of blood components into the tissues and is largely responsible for primary signal transmission in regulating vascular tone. The middle layer, the *tunica media*, contains the fibrous structural protein elastin, arranged in helical lamellae interspersed with collagen, smooth-muscle cells (SMCs), and some fibroblasts. The aortic media also contains a gel of proteoglycans and glycoproteins (collectively termed ground substance). It is the medial layer that provides the greatest amount of mechanical integrity to the aortic wall. The outermost layer, the *tunica adventitia*, is composed of loose con-

Supported by National Institutes of Health/National Heart, Lung, and Blood Institute grant R01 HL075488-05 and a Career Development Award (BLRD-CDA-2) from the Department of Veterans Affairs.

Accepted for publication July 2, 2009.

Address reprint requests to Jeffrey A. Jones, Ph.D., Division of Cardiothoracic Surgery Research, Department of Surgery, Medical University of South Carolina, Strom Thurmond Research Building, 114 Doughty Street, Suite 625, Charleston, SC 29425. E-mail: jonesja@musc.edu.

nective tissue, collagen, and elastin fibers (nonlamellar) and is the primary reservoir for fibroblasts. The adventitia contributes highly to the structural integrity of the aorta.

In clinical aneurysm specimens, remodeling of the structural proteins is accompanied by changes in cellular content.[8–11] We therefore hypothesized that as TAA development progresses, the medial SMC content within the aortic wall would decrease, leaving the fibroblast as the predominant cell type to manage the vascular remodeling process. Thus, using an established murine model of TAA, the present study had two objectives. First, histologically assess the structural and compositional changes in aortic collagen and elastin content over the first 16 weeks following TAA induction. The second objective was to determine the changes in cellular content over the same time course, using cell-type-specific marker proteins to identify and quantitate the medial cellular constituents. Taken together, this unique longitudinal study will establish a temporal framework that will allow the changes in cellular constituents to be coordinated with alterations in aortic structure.

Materials and Methods

Experimental Design

The present study examined a total of 20 C57BL/6J mice (composed of approximately equal number of males (55%) and females (45%)). Of five experimental groups ($n = 4$ in each group), four underwent TAA induction surgery with terminal time points of 2-, 4-, 8-, and 16-weeks post-TAA induction. The descending thoracic aorta of each mouse was excised and processed for histological assessment of structural proteins (collagen and elastin) and cellular constituents (fibroblasts, myofibroblasts, and SMCs) and inflammatory infiltrate (macrophages and neutrophils). Results were compared with unoperated mice (no TAA induction; $n = 4$), which served as a reference control group. All animals were 8 to 12 weeks of age at time of surgical TAA induction. This animal protocol was approved by the Medical University of South Carolina Institutional Animal Care and Use Committee (ARC no. 2146), and all mice were treated and cared for in accordance with the National Institutes of Health *Guide for the Care and Use of Laboratory Animals* (NIH Publication No. 85-23, revised 1996).

Operative Procedure

Murine TAAs were induced as described previously.[12] Briefly, following anesthetic induction, mice were intubated, and a surgical plane of anesthesia was maintained by nosecone with a 2% isoflurane/oxygen mixture. The descending thoracic aorta was exposed through a left thoracotomy, and the baseline aortic outer diameter was measured by video micrometry and recorded as described previously.[13] A sponge soaked in 0.5 M calcium chloride was then placed in direct contact with the periadventitial surface for 15 minutes. The chest was closed in layers, and the mice were allowed to recover.

Terminal Surgical Procedures and Aortic Perfusion-Fixation

At time of terminal surgery, the descending thoracic aorta was re-exposed and terminal aortic outer diameter measurements were recorded. The isoflurane mixture was then increased to 5%, and mice were euthanized under deep anesthesia by exsanguination induced by right atriotomy. The aorta was then perfused (via a *trans*-ventricular needle) with 0.9% sterile saline at a pressure of 100 mm Hg. The perfusate was allowed to escape through the right atriotomy and continued until the perfusate was clear, and the liver was blanched indicating no remaining blood. To maintain the aortic ultrastructure, the animal was then systemically perfused with 10% formalin in PBS for 3 minutes at 100 mm Hg, followed by complete successive submersion in 10% formalin for 48 hours and 70% ethanol for 24 hours, at 4°C. The descending thoracic aorta was then carefully excised and sharply bisected at the site of TAA induction. Each half of the aorta was then paraffin-embedded on end, and 3-μm-thick cross-sections were cut and mounted on glass slides. Every 10th section was stained with H&E to verify the site of TAA induction. All subsequent sections used for histochemical and immunohistochemical analysis were located within the calcium chloride treated region of the thoracic aorta.

Microscopy

Microscopic images of aortic tissue sections were visualized on a Zeiss Axioskop 2 microscope (Carl Zeiss MicroImaging, Thornwood, NY) using a 63X/1.25 Plan-NEOFLUAR oil objective and acquired using an Axiocam MRc color charge-coupled device camera connected to a computer running AxioVision Software release version 4.6. All subsequent image analysis was performed using SigmaScanPro v5.0 (SPSS, Chicago, IL).

Collagen Analysis (Picrosirius Red Staining)

Aortic tissue sections were placed in 0.2% phosphomolybdic acid for 5 minutes, and rinsed with two changes of distilled water. Total collagen was then stained by placing the slides in a 1% solution of picrosirius red for 90 minutes with subsequent destaining through three changes of 0.01 N HCl. Aortic collagen content was determined by imaging stained aortic sections under high magnification illuminated by polarized light.[14] The percent area of collagen staining was quantitated by comparing the area of birefringent signal to the total area of the aortic media or adventitia.

Elastin Analysis (Luna Staining)

Elastin content in the aortic media was quantitated using the Luna staining technique. Aortic tissue sections were stained in aldehyde fuchsin solution for 30 minutes and differentiated through three changes of 95% alcohol. Aortic medial elastin content was determined by imaging

stained aortic sections under high magnification and quantitating 1) the number of unbroken elastic lamellae per high-power field by direct count, 2) the percent area of elastin as compared with total medial tissue area, and 3) the percent area of the medial components between the elastic lamellae (gap area) as compared with the total medial tissue area. Changes in medial thinning and aortic stiffness[15,16] were then estimated at each time point from the ratio of gap area to elastin area, and total collagen area to total elastin area, respectively.

Immunohistochemistry

The cellular constituents within the aortic media were identified and quantitated using immunohistochemical techniques with antibodies that recognized cell-type-specific marker proteins. Aortic tissue sections were incubated in DakoCytomation Antigen Retrieval Solution (catalog no. S1699; DakoCytomation, Carpinteria, CA) for 30 minutes at 99°C. The sections were allowed to cool to room temperature and were washed three times for 2 minutes in PBS, followed by two times for 2 minutes in Tris-buffered saline containing 0.025% Triton X-100 (Tris-buffered saline wash solution). The tissue sections were then incubated in blocking solution (3% bovine serum albumin in Tris-buffered saline wash solution) for 2 hours at room temperature, followed by overnight incubation at 4°C with cell-type-specific primary antibodies diluted in blocking solution. Cell-type-specific antisera were used to identify: 1) fibroblasts (goat anti-discoidin domain receptor 2 (DDR2), 1:100, no. SC-7555; Santa Cruz Biotechnology, Santa Cruz, CA); 2) SMCs/myofibroblasts (rabbit anti-smooth muscle myosin heavy chain 2 (Myh11), 1:100, no. ab53219; Abcam, Cambridge, MA); 3) SMCs/myofibroblasts (rabbit anti-α-smooth-muscle actin (α-SMA), 1:100, no. ab5694; Abcam); 4) SMCs (rabbit anti-desmin, 1:20, D8281; Sigma-Aldrich, St. Louis, MO); 5) macrophages (rat anti-MAC3, 1:10, no. 550292; BD Pharmingen, San Diego, CA); and 6) neutrophils (rat anti-CD11b, 1:40, no. ab6332; Abcam). The slides were then washed with PBS and incubated in 3% H_2O_2/PBS for 30 minutes at room temperature to block endogenous peroxidase activity. The sections were then allowed to incubate with primary antibody species-specific peroxidase-conjugated secondary antibodies (VectaStain ABC Elite anti-rat (no. 6104), anti-rabbit (no. 6101), or anti-goat (biotinylated, no. BA-5000), or VectaStain ABC-AP anti-rabbit (no. AK-5001); Vector Laboratories, Burlingame, CA). Positive immune reactions were visualized by incubating the sections with 0.05% diaminobenzidine in PBS containing 0.015% H_2O_2, which formed a brown precipitate on reaction with the peroxidase enzyme, or in the case of the ABC-AP secondary, the Vector Blue (no. SK-5300; Vector Laboratories) chromagen was used. Serial sections were used for negative controls and were processed in the same fashion but without the addition of primary antisera. Tissue sections from lung, intestine, or myocardium were used as positive controls to verify antisera-antigen interactions.

Detection of Apoptotic Cells

Aortic sections from each time-point were analyzed by immunohistochemistry to identify early apoptotic cells using an antibody specific for activated caspase-3 (p17 fragment).[17–19] Aortic tissue sections were incubated in antigen retrieval solution and processed as described above. The sections were then washed and incubated in blocking solution (3% bovine serum albumin in Tris-buffered saline wash solution) for 2 hours at room temperature, followed by overnight incubation at 4°C with an antibody specific for activated caspase-3 (rabbit anti-caspase-3, 1:50, no. ab2302; Abcam) diluted in blocking solution. The following day the slides were washed, and endogenous peroxidase activity was blocked as described above. The sections were then allowed to incubate with peroxidase-conjugated secondary antibody (VectaStain ABC Elite, anti-rabbit (no. 6101); Vector Laboratories) for 1 hour at room temperature. Positive immune reactions were visualized by incubating the sections with 0.05% diaminobenzidine in PBS containing 0.015% H_2O_2, as before. For localization of desmin and activated caspase-3, serial sections were stained and imaged as described above.

Data Analysis

Change in aortic diameter was expressed as a percentage change from mean baseline size within each treatment group. For the analysis of collagen content, three independent images were obtained from three sections spaced at approximately 30-μm intervals in each mouse from each treatment group and were analyzed independently for adventitial versus medial collagen content. The amount of collagen from each image was averaged per section. A mean of three sections was then computed as the average collagen content per animal. The change in collagen content between treatment groups (control, $n = 4$; 2-week post-TAA, $n = 4$; 4-week post-TAA, $n = 4$; 8-week post-TAA, $n = 4$; and 16-week post-TAA, $n = 4$) was determined and subjected to statistical analysis. For the analysis of elastin content and structure, a single image obtained from three sections spaced at approximately 30-μm intervals in each mouse from each treatment group was analyzed to determine the number of elastic lamellae, the total elastin area, and total gap area. A mean of each parameter was computed for each animal. The change in parameters between treatment groups (control, $n = 4$; 2-weeks post-TAA, $n = 4$; 4-weeks post-TAA, $n = 4$; 8-weeks post-TAA, $n = 4$; and 16-weeks post-TAA, $n = 4$) was determined and subjected to statistical analysis. For the quantitation of specific cell types within the aortic media, three independent images were acquired from two sections spaced approximately 30 μm apart, in each mouse from each treatment group. Cell type was analyzed by directly counting the number of cells staining positive for a particular cell-type marker in each high-power field. Counting was performed by two independent observers (J.A.J. and C.B.), and any results with a coefficient of variance $>25\%$ were reanalyzed.

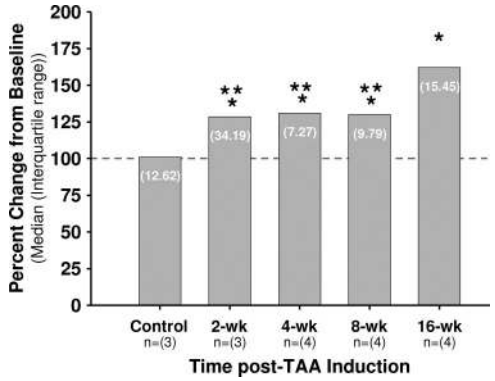

Figure 1. Change in aortic diameter over time post-TAA induction. Median aortic diameter was increased over baseline (average baseline value = 655.3 μm) at each time point post-TAA induction, and diameters in the 2-, 4-, and 8-week groups were different from the 16-week group. Bars represent median aortic diameter; numbers in parentheses are interquartile ranges (25 to 75%). Statistical analysis: Kruskal-Wallis ($P = 0.0291$); Mann-Whitney (*$P < 0.05$ versus baseline, **$P < 0.05$ versus 16-week TAA).

Cells possessing positive immunoreactivity were counted using SigmaScan Pro version 5.0 (SPSS). Color inversion was used to enhance and confirm positive staining and cellularity. The number of cells (marker-specific) from each image was averaged for each section. A mean of the two sections was then computed as the average number of cells per animal. The change in cell number between treatment groups (control, $n = 4$; 2-week post-TAA, $n = 4$; 4-week post-TAA, $n = 4$; 8-week post-TAA, $n = 4$; and 16-week post-TAA, $n = 4$) was then determined and subjected to statistical analysis. In each case, results were expressed as a median and an interquartile range (indicated in parentheses on each bar graph).

All statistical procedures were performed using the Stata statistical package (Intercooled Stata version 8.2; StataCorp LP, College Station, TX). Comparisons between time points post-TAA induction were made using Kruskal-Wallis followed by a nonpaired Mann-Whitney rank sum test; $P < 0.05$ was considered significant.

Results

Aortic Diameter Measurements

Aortic diameter measurements revealed an increase in median aortic diameter, as compared with baseline, at each time point post-TAA induction (Figure 1). Median aortic dilatation reached a maximum of 62% at 16 weeks, consistent with TAA development.

Collagen Analysis

Total collagen content was measured in aortic tissue sections in both the adventitial and medial regions independently. No changes in collagen content were observed over the 16-week time course post-TAA induction (Figure 2, A and B).

Elastin Analysis

Aortic tissue sections from TAA and control mice were stained with aldehyde fuchsin (Luna stain; Figure 3A). The number of unbroken elastic lamellae, the area fraction of Luna staining, and the gap area between elastic lamellae were subsequently quantitated. The results revealed a decrease in the number of unbroken elastic lamellae at all time points post-TAA induction, ranging from a median of 6 in the reference control group to a nadir of 3.9 at 8 weeks (Figure 3B). The area fraction of elastin within the aortic media was then determined and found to be significantly elevated at 4-weeks post-TAA induction and significantly decreased at 16 weeks, with no difference from control measured at 2 and 8 weeks (Figure 3C). The gap area between elastic lamellae was significantly decreased from control at 4-weeks post-TAA induction (Figure 3D).

Structural Analysis

The ratio of gap area to elastin area revealed a significant decrease in aortic medial thickness at 4-weeks post-TAA induction, followed by an increase at 16 weeks (Figure 4A). Aortic stiffness was estimated by the ratio of total collagen to elastin and revealed a significant increase in aortic stiffness at 8- and 16-weeks post-TAA induction, with a trend toward increased stiffness at 2 weeks (Figure 4B).

Analysis of Cellular Constituents

To define the changes in cellular makeup within the aortic wall during TAA formation, aortic sections from control and TAA-induced mice were stained for cell-type-spe-

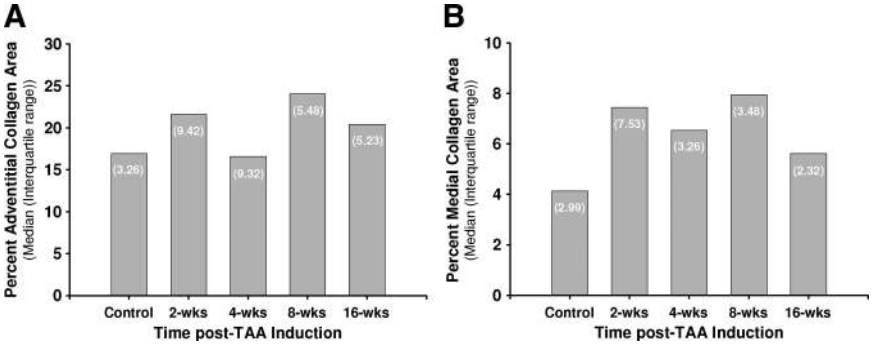

Figure 2. Analysis of medial and adventitial collagen content. Collagen content was measured in aortic tissues from control and TAA-induced mice. Picrosirius red-stained sections were illuminated with polarized light and the resulting birefringence was quantitated in the aortic adventitia (**A**) and aortic media (**B**). No significant changes in collagen content were observed. Treatment groups: control ($n = 4$), 2 weeks ($n = 4$), 4 weeks ($n = 3$), 8 weeks ($n = 4$), and 16 weeks ($n = 4$). Bars represent median values; numbers in parentheses are interquartile ranges (25 to 75%). Statistical analysis: Kruskal-Wallis (**A**, $P = 0.3696$; **B**, $P = 0.3302$).

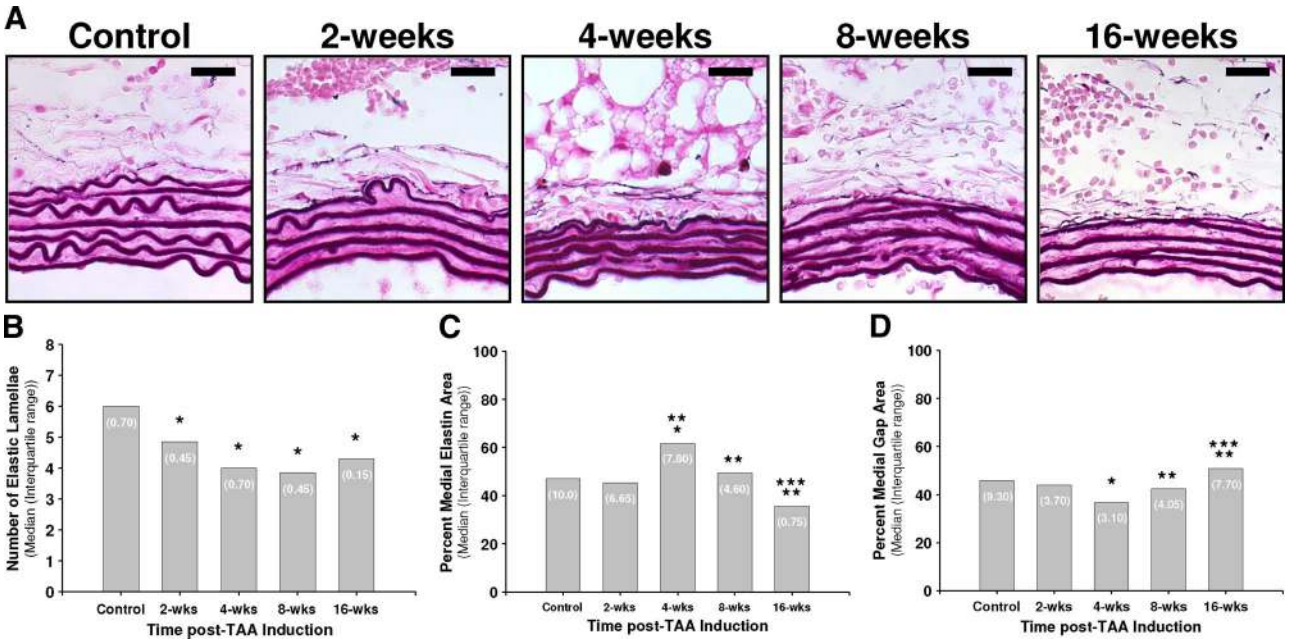

Figure 3. Analysis of medial elastin content and architecture. The medial elastin content and architecture were analyzed in aortic tissues from control and TAA-induced mice. **A:** Representative Luna-stained sections showing architectural changes over time post-TAA induction; scale bar is equal to 20 μm. **B:** The number of unbroken elastic lamellae were quantitated at each time point post-TAA induction, Kruskal-Wallis ($P = 0.0102$). **C:** The medial area fraction of elastin content was quantitated at each time point post-TAA induction, Kruskal-Wallis ($P = 0.0110$). **D:** The gap area between elastic lamellae was quantitated at each time point post-TAA induction, Kruskal-Wallis ($P = 0.0136$). Treatment groups: control ($n = 4$), 2 weeks ($n = 4$), 4 weeks ($n = 3$), 8 weeks ($n = 4$), and 16 weeks ($n = 4$). Bars represent median values; numbers in parentheses are interquartile ranges (25 to 75%). Statistical analysis: Mann-Whitney (*$P < 0.05$ versus control, **$P < 0.05$ versus 4-week, and ***$P < 0.05$ versus 8-week).

cific marker proteins (Figure 5), and cell numbers were quantitated at each time point by direct counting. The data revealed an increase in the number of DDR2$^+$ cells (fibroblasts) at 8- and 16-weeks post-TAA induction (Figure 6A). Similarly, the number of Myh11$^+$ cells (SMCs/myofibroblasts) was also elevated at 8- and 16-weeks post-TAA induction (Figure 6B), whereas the number of α-SMA$^+$ cells (SMCs/myofibroblasts) did not change significantly from control throughout the time course (Figure 6C). The number of desmin$^+$ cells (SMCs) was significantly elevated at 4-weeks post-TAA induction but was not different from control levels at the other time points (Figure 6D). Minimal staining was observed for MAC3 (macrophages) and CD11b (neutrophils), and no change was observed over the time course of the study (data not shown).

Analysis of Apoptosis

To determine the extent of apoptosis that occurred over the time course of TAA formation, aortic sections from control and TAA-induced mice were stained for the active fragment (p17) of caspase-3 (Figure 7A). The data revealed enhanced apoptosis at 8- and 16-weeks post-TAA induction. When serial sections from a 16-week TAA were stained for active caspase-3 and desmin (SMC marker), significant overlap was observed, suggesting that SMCs were actively undergoing apoptotic cell death (Figure 7B).

Discussion

Dysregulation of physiological vascular remodeling within the aortic wall can result in excessive deposition or

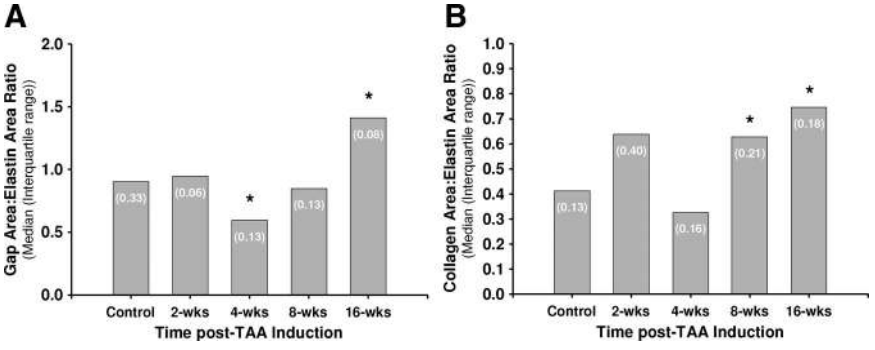

Figure 4. Analysis of medial thinning and aortic stiffness over time post-TAA induction. **A:** Aortic medial thinning was approximated by calculating the ratio of gap area to elastin area, Kruskal-Wallis ($P = 0.0087$). **B:** Aortic stiffness was approximated by calculating the ratio of total collagen area to elastin area, Kruskal-Wallis ($P = 0.0978$). Treatment groups: control ($n = 4$), 2 weeks ($n = 4$), 4 weeks ($n = 3$), 8 weeks ($n = 4$), and 16 weeks ($n = 4$). Bars represent median values; numbers in parentheses are interquartile ranges (25 to 75%). Statistical analysis: Mann-Whitney (*$P < 0.05$ versus control).

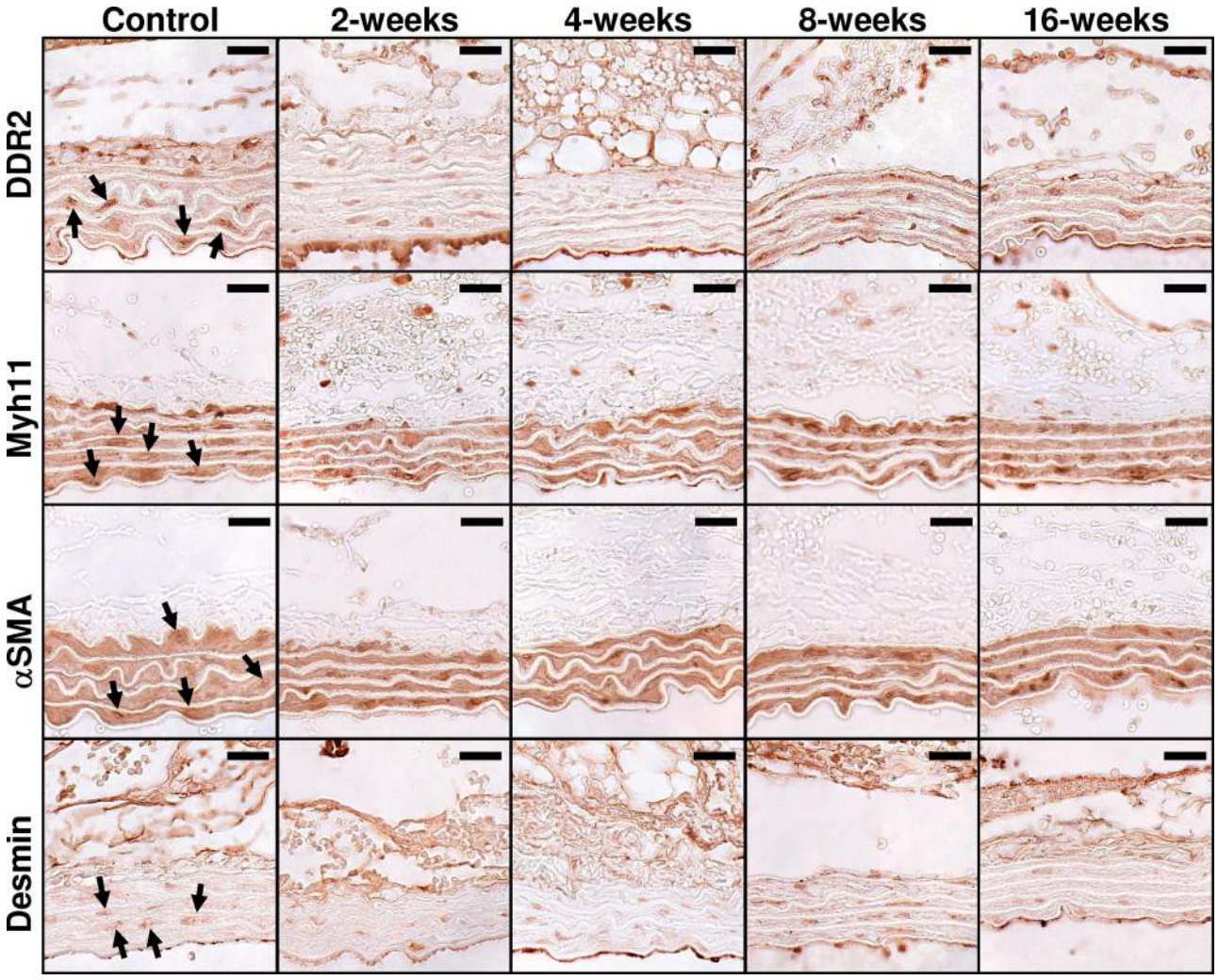

Figure 5. Immunohistochemical results for cell-type-specific marker proteins in aortic sections over time post-TAA induction. Aortic tissue sections from and control and TAA-induced mice were stained with cell-type-specific antibodies for fibroblasts (DDR2), SMCs/myofibroblasts (α-SMA and Myh11), and SMCs (desmin). The **arrows** point to representative cells selected as having positive staining. Color inversion was used to verify cellularity and increased staining intensity over background. Scale bar equals 20 μm.

degradation of critical ECM components, thereby altering the mechanical strength and integrity of the aorta, and increasing the potential for dissection or dilatation. Although degradation of the primary structural components, collagen and elastin, is a common feature of aortic aneurysms undergoing vascular remodeling,[20–22] a comprehensive analysis of the changes in cellular composition during TAA development has not been performed. Accordingly, the present study set out to define the coordinate changes in aortic structure and endogenous cellular composition at the histological level over the course of TAA development in an established murine model. We hypothesized that alterations in aortic collagen and elastin content would coincide with a change in cellular constituents, promoting the fibroblast as the predominant endogenous cell type within the aortic wall and thereby elevating its functional importance in mediating the vascular-remodeling process. The unique findings of the present study were twofold. First, aortic dilatation proceeded secondary to changes in aortic elastin content and organization, whereas collagen levels remained unchanged. Second, the changes in aortic architecture were accompanied by the emergence of a subset of cells that possessed both fibroblast- and SMC-specific marker proteins. Taken together, these data suggest that a subset of phenotypically unique endogenous cells, characteristic of myofibroblasts, may play a critical role in mediating the alterations in aortic structure and composition during TAA development. Targeting myofibroblast differentiation may therefore have significant implication toward regulating TAA formation and progression.

Analysis of TAA-Induced Structural Changes

Previous studies examining clinical specimens have suggested that alterations in collagen content play a direct role in aneurysm development.[23–25] The present study, however, revealed no significant change in either the adventitial or medial collagen content during TAA formation. Although this may suggest a lack of collagen degradation, given previous results establishing a temporal

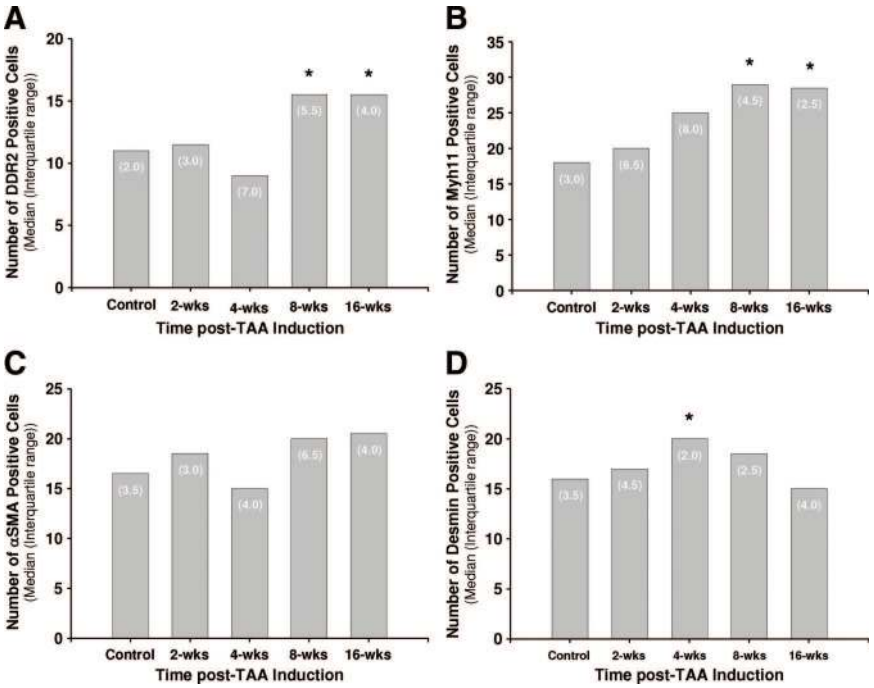

Figure 6. Quantitation of immunohistochemical staining results for cell-type-specific marker proteins. The median number of positively stained cells in each aortic tissue section from control and TAA-induced mice was determined for each cell-type-specific marker protein: fibroblasts (DDR2), Kruskal-Wallis ($P = 0.0122$, **A**); SMCs/myofibroblasts (Myh11), Kruskal-Wallis ($P = 0.0216$, **B**); SMCs/myofibroblasts (α-SMA), Kruskal-Wallis ($P = 0.2667$, **C**); and SMCs (desmin), Kruskal-Wallis ($P = 0.0916$, **D**). Treatment groups: control ($n = 4$), 2 weeks ($n = 4$), 4 weeks ($n = 3$), 8 weeks ($n = 4$), and 16 weeks ($n = 4$). Bars represent median values; numbers in parentheses are interquartile ranges (25 to 75%). Statistical analysis: Mann-Whitney (*$P < 0.05$ versus control).

profile of protease production throughout TAA development,[26] it is more likely that collagen degradation and deposition remain balanced in regard to total content. Organizational structure, on the other hand, may be significantly affected by the induced remodeling process, as has previously been defined during myocardial remodeling.[27,28]

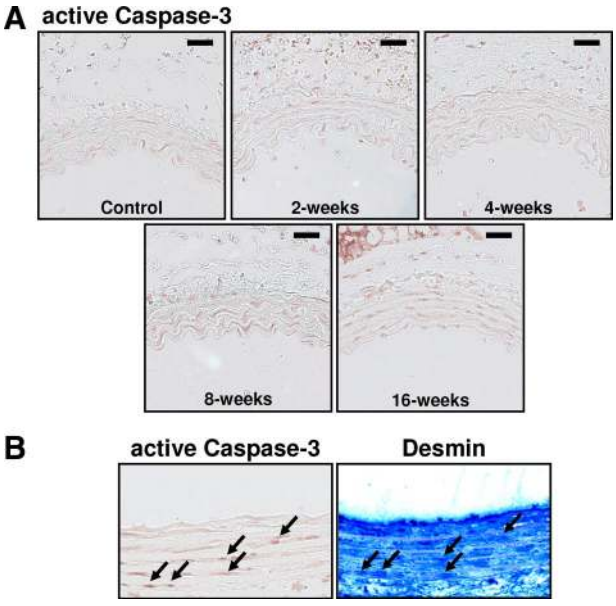

Figure 7. Immunostaining for apoptotic cells. **A:** Tissue sections from control and TAA-induced mice were immunostained for the active fragment of caspase-3 (p17) demonstrating enhanced apoptosis at 8- and 16-week post-TAA induction. **B:** Serial tissue sections from a 16-week TAA were stained with antibodies for apoptotic cells (active caspase-3) or SMCs (desmin). The **arrows** indicate cells staining for both active caspase-3 and desmin on serial sections. Taken together, these results suggest that a portion of the SMC population undergoes apoptosis during TAA formation.

Unlike total collagen content, the early stages of aortic dilatation were characterized by thinning and flattening of the medial elastic lamellae evident as early as 2-week and persisting throughout 16-week post-TAA induction. This observation was consistent with previous studies from our laboratory and others.[13,29] Accordingly, several measures were used to assess changes in the elastic architecture. First, the numbers of unbroken elastic lamellae were quantitated at each time point by direct counting. Results from the present study demonstrated a progressive decrease in the number of unbroken elastic lamellae from six in the control sections to four at 8-weeks post-TAA induction. Second, total elastin content was estimated from the area fraction of elastin staining within the aortic media. The percent medial elastin area increased from control at 4-weeks post-TAA induction, decreased back to control levels at 8 weeks, and reached a minimum at 16-weeks post-TAA induction. The data from the later time points are reflective of elastolysis within the aortic media and represent the likely cause for aortic dilatation. Third, in addition to changes in the elastic lamellar architecture and content, the matrix between the lamellae also dynamically changed throughout the TAA time course. The "gap area" was significantly decreased at 4-week post-TAA induction and then progressively increased from 4 through 16 weeks, returning to control levels. This region of the aortic media contains SMCs, some fibroblasts, and a rich ECM composed of collagen, proteoglycans, and various glycoproteins. Although the change in total medial collagen was shown to be minimal, the reduction in gap area may be driven by a loss in both the cellular content (discussed below) as well as proteoglycan matrix. This is supported by Kowalewski et al,[30] demonstrating elevated activity of proteoglycan degrading enzymes in abdominal aortic aneurysm specimens.

This may suggest that significant proteoglycan degradation contributes to the medial atrophy observed during TAA formation.

To further define the changes in elastic architecture, an estimate of medial thinning was calculated as a function of the ratio of "gap area" to elastin area. The results demonstrate a significant decrease in medial thickness at 4-weeks post-TAA induction, which recovered to control levels by 8 weeks, and was increased over control levels at 16-weeks post-TAA induction. Although medial thinning and flattening was apparent at the microscopic level, the increase in medial elastin area measured at 4 weeks was most likely explained by the decrease in total medial area. In the same fashion, as the gap area recovered, the total medial elastin area continued to decrease between 4 and 16 weeks, confirming elastolysis at the later time points.

Taken together, these measures confirm enhanced degradation of the elastic lamellae, which is highly consistent with the advanced aortic remodeling expected during aneurysm development. Moreover, these results also demonstrated changes in medial aortic dimension consistent with the loss of structural components between the elastic lamellae. Interestingly, although the medial area recovered in thickness between 4 and 16 weeks, the area fraction of elastin remained depressed. This suggests that there is enhancement of matrix deposition to compensate for the loss of structural integrity. This would also suggest that a cellular component within the aortic media is activated within this timeframe to induce ECM synthesis and deposition.

Because aortic compliance and resiliency depend on both collagen and elastin content, aortic stiffness is likely affected in response to alterations in the elastic architecture. Accordingly, aortic stiffness was estimated from the ratio of collagen area to elastin area, as described previously.[15,16] These results demonstrated increased aortic stiffness at 8- and 16-weeks post-TAA induction, with a trend toward increased stiffness at 2 weeks. Although the measured increase in stiffness is most likely driven by the loss of elastin at the later time points, increased stiffness may signal a dynamic shift in medial homeostasis, resulting in a compensatory production of proteolytic enzymes that could further exacerbate the architectural changes in the aortic media. These results further suggest that there is a delicate balance between matrix synthesis and degradation and that both processes may be temporally activated throughout aneurysm development.

Analysis of TAA-Induced Cellular Constituents

In addition to the changes in structural protein content, TAA development is also accompanied by changes in the cellular constituents within the aortic vascular wall. Multiple studies have suggested that apoptosis of SMCs is a key determinant of medial degeneration in both thoracic[8,9] and abdominal[10,11] aortic aneurysms. Using cell-type-specific protein markers the cellular constituents, both infiltrating and endogenous, were determined within the aortic wall during TAA formation.

The presence of macrophages and neutrophils were assessed in aortic tissue sections by staining with antibodies against MAC3[31] and Cd11b,[32] respectively. Consistent with previous results from this laboratory demonstrating minimal inflammatory infiltrate through 4-week post-TAA induction,[13] no change in the number of macrophages or neutrophils was observed through 16 weeks. These results support the hypothesis that alterations in the endogenous cellular constituents are responsible for the altered matrix metalloproteinase levels observed during TAA formation.

To determine changes in the endogenous cellular constituents within the aortic media, four cell-type-specific marker proteins were chosen to define the independent cellular populations. Fibroblasts were identified using antibodies specific for the collagen receptor, DDR2. DDR2 has previously been shown to display fibroblast-restricted expression and, in cardiovascular tissues, has proven to be a better marker for fibroblasts than the fibroblast-specific protein-1.[33] Likewise, SMCs were identified using antibodies against desmin, a 52-kDa intermediate filament protein specifically found in muscle-derived cells, including SMCs.[34–36] To further define the SMC population and to identify the presence of myofibroblasts, antibodies against α-SMA and smooth-muscle myosin heavy chain (SM2 or Myh11) were also used.[37,38] Results from the present study demonstrated an increase in the number of DDR2$^+$ cells at 8- and 16-weeks post-TAA induction, suggesting an increase in the number of fibroblasts or fibroblast-derived cells at these time points. Interestingly, this occurred concomitantly with an increase in smooth-muscle myosin staining (Myh11). The elevated myh11 would suggest an expansion of SMCs or myofibroblasts. Accordingly, to further differentiate between these two cell types, serial tissue sections were stained for the intermediate filament desmin. Previous studies have established that desmin$^+$ staining is clearly associated with SMCs and is rarely found in fibroblasts or myofibroblasts.[35,39] The present data revealed a peak in desmin$^+$ staining at 4-weeks post-TAA induction, followed by a decrease in desmin$^+$ cells through 16 weeks. As a second measure of SMCs and myofibroblasts, tissue sections were then stained with antibodies against α-SMA, a well described marker for SMCs and myofibroblasts. Interestingly, α-SMA$^+$ cells remained unchanged throughout the 16-week time course (summarized in Figure 8). Taken together, these unique results suggest that aortic dilatation occurs simultaneously with the emergence of a population of fibroblast-derived myofibroblasts that stain positive for DDR2/Myh11/α-SMA and negative for desmin. The unchanged number αSMA$^+$ cells is not surprising given that SMC apoptosis has been associated with aneurysm formation.[8–11] As such, SMCs (defined by desmin/α-SMA$^+$ staining) may be decreasing in number at the same time as myofibroblasts (defined by DDR2/Myh11/α-SMA$^+$ staining) are increasing. Thus, the overall number of α-SMA$^+$ cells would likely fall somewhere in between, and our results are consistent with this suggestion.

To determine whether SMCs were indeed undergoing apoptosis, tissue sections from control and TAA-induced

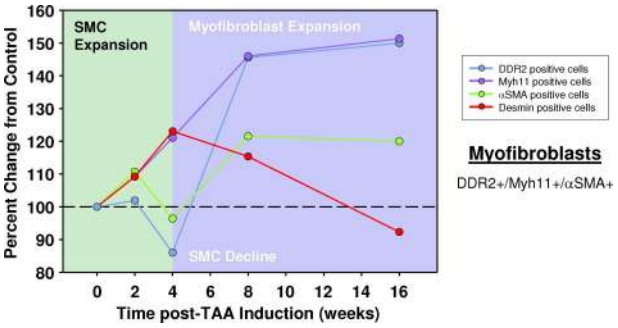

Figure 8. Summary of cell-type-specific changes over time post-TAA induction. The number of cells staining positive with a specific cell-type marker were expressed as a percent change from control to show relative changes in medial cellular makeup over the course of TAA development. The results demonstrate an increase in the number of DDR2/Myh11/α-SMA$^+$ cells, and a decrease in the number of desmin/α-SMA$^+$ cells, suggesting the emergence of a population of fibroblast-derived myofibroblasts between 4- and 16-week post-TAA induction.

mice were immunostained for the active fragment (p17) of caspase-3. Like all caspases, the active enzyme is maintained in an inhibited form until released by proteolysis. The presence of the p17 fragment indicates specific activation of caspase-3, which has been clearly established as a marker of early apoptosis.[17–19] The present study demonstrated enhanced active caspase-3 staining in tissue sections from 8- and 16-week TAA-induced mice. Moreover, when serial sections of a 16-week TAA were stained with antibodies for active caspase-3, or the SMC marker desmin, significant overlap was observed, suggesting that the population of dying cells were SMCs. These results are consistent with the decrease in desmin$^+$ cells observed at the later time points.

The myofibroblast constitutes a unique cell type, which arises through a specific differentiation process and possesses characteristics of both fibroblasts and SMCs. Previous studies have demonstrated that myofibroblasts play a significant role in the tissue injury response.[40,41] Accordingly, they have the ability to migrate to the site of injury, where they can produce critical matrix proteins and participate in wound contracture/stabilization. Identification of myofibroblasts can be difficult because of their ability to differentially express several cell-type-specific marker proteins.[36,42] In almost all cases, when assessing tissues that do not contain SMCs, α-SMA is the primary marker used to reliably identify myofibroblasts. In the aortic wall, however, α-SMA$^+$ staining can represent both vascular SMCs and myofibroblasts. Accordingly, the present study used additional marker proteins (Myh11 and desmin) to distinguish between the two cell types.[36] Although positive Myh11 staining in vascular tissues does not constitute a definitive myofibroblast marker alone, as it too can be expressed by some SMCs, the decrease in desmin$^+$ cells accompanied by the increase in Myh11$^+$ cells provided the necessary differential to distinguish between SMCs and myofibroblasts. Accordingly, the present data identify the emergence of a population of fibroblast-derived myofibroblasts that may contribute to the changes in the vascular ECM during TAA development.

Although the role of myofibroblast differentiation has previously been established in the myocardium following ischemic injury,[43] and myofibroblasts have been identified in a rare subset of inflammatory abdominal aortic aneurysms,[44] this is the first study to suggest myofibroblast involvement in TAA formation. Interestingly, transforming growth factor-β is a known regulator of myofibroblast differentiation.[45,46] Previous studies from this laboratory have identified altered transforming growth factor-β signaling in aortic tissue from TAA-induced mice.[47] Thus, it is interesting to speculate that alterations in transforming growth factor-β signaling may contribute to TAA development through the induction of myofibroblast differentiation within the aortic wall. Moreover, the myofibroblast population appears to emerge around the 4-week time point, coinciding with the decrease in medial proteoglycan content, a reservoir known to sequester latent growth factors, including transforming growth factor-β.[48,49]

Taken together, the present study identifies the myofibroblast as a critical cell type within the aortic wall that is capable of modulating the ECM remodeling process. What remains unknown is whether myofibroblast differentiation is induced to repair the damaged aortic wall or whether its presence further exacerbates pathological remodeling. Additional studies targeting myofibroblast differentiation will be required to determine the functional role of this interesting cell type in TAA development.

Limitations

The present study is not without limitations. First, collagen and elastin content were quantitated using histochemical staining procedures. Although these staining methods are well established, quantitation of these proteins can be difficult using morphometric techniques. However, because both collagen and elastin exist in a soluble and insoluble form, as well as a pro- and processed form, morphometric analysis is still the best method for quantitating collagen and elastin deposition in the ECM. Second, aortic stiffness was estimated based on the ratio of collagen to elastin and did not take into account the degree of collagen cross-linking. Third, cell-type identification by staining for specific marker proteins represents a challenging endeavor, particularly for cell types that are classically difficult to distinguish like fibroblasts and SMCs. Although the present study describes the emergence of a unique population of cells that are consistent with the myofibroblast phenotype, it remains to be determined whether this is the result of the recruitment and migration of differentiated adventitial fibroblasts or the clonal expansion of a differentiating resident medial fibroblast. Last, significant gender interactions with respect to change in aortic diameter could not be demonstrated, and therefore, data from both male and female mice were pooled for analysis in this study. It remains to be established whether gender-dependent differences exist in aortic cellular profiles. These issues will be addressed in future studies.

Limitations notwithstanding, this unique longitudinal study has established a temporal framework in which the

changes in aortic structural components can be placed in context with alterations in aortic cellular composition. As such, these unique results suggest the emergence of a population of fibroblast-derived myofibroblasts that may play a significant role in TAA development through the enhancement of ECM proteolysis. Targeting myofibroblast differentiation may therefore have significant implications toward regulating TAA formation and progression.

References

1. Coady MA, Rizzo JA, Goldstein LJ, Elefteriades JA: Natural history, pathogenesis, and etiology of thoracic aortic aneurysms and dissections. Cardiol Clin 1999, 17:615–635
2. Isselbacher EM: Thoracic and abdominal aortic aneurysms. Circulation 2005, 111:816–828
3. Barbour JR, Spinale FG, Ikonomidis JS: Proteinase systems and thoracic aortic aneurysm progression. J Surg Res 2007, 139:292–307
4. Koullias GJ, Ravichandran P, Korkolis DP, Rimm DL, Elefteriades JA: Increased tissue microarray matrix metalloproteinase expression favors proteolysis in thoracic aortic aneurysms and dissections. Ann Thorac Surg 2004, 78:2106–2110; discussion 2110–2101
5. Dingemans KP, Teeling P, Lagendijk JH, Becker AE: Extracellular matrix of the human aortic media: an ultrastructural histochemical and immunohistochemical study of the adult aortic media. Anat Rec 2000, 258:1–14
6. Wolinsky H, Glagov S: A lamellar unit of aortic medial structure and function in mammals. Circ Res 1967, 20:99–111
7. Jacob MP, Badier-Commander C, Fontaine V, Benazzoug Y, Feldman L, Michel JB: Extracellular matrix remodeling in the vascular wall. Pathol Biol 2001, 49:326–332
8. Della Corte A, Quarto C, Bancone C, Castaldo C, Di Meglio F, Nurzynska D, De Santo LS, De Feo M, Scardone M, Montagnani S, Cotrufo M: Spatiotemporal patterns of smooth muscle cell changes in ascending aortic dilatation with bicuspid and tricuspid aortic valve stenosis: focus on cell-matrix signaling. J Thorac Cardiovasc Surg 2008, 135:8–18, 18 e11–12
9. Ihling C, Szombathy T, Nampoothiri K, Haendeler J, Beyersdorf F, Uhl M, Zeiher AM, Schaefer HE: Cystic medial degeneration of the aorta is associated with p53 accumulation, Bax upregulation, apoptotic cell death, and cell proliferation. Heart 1999, 82:286–293
10. Lopez-Candales A, Holmes DR, Liao S, Scott MJ, Wickline SA, Thompson RW: Decreased vascular smooth muscle cell density in medial degeneration of human abdominal aortic aneurysms. Am J Pathol 1997, 150:993–1007
11. Thompson RW, Liao S, Curci JA: Vascular smooth muscle cell apoptosis in abdominal aortic aneurysms. Coron Artery Dis 1997, 8:623–631
12. Ikonomidis JS, Gibson WC, Gardner J, Sweterlitsch S, Thompson RP, Mukherjee R, Spinale FG: A murine model of thoracic aortic aneurysms. J Surg Res 2003, 115:157–163
13. Jones JA, Barbour JR, Lowry AS, Bouges S, Beck C, McClister DM, Jr., Mukherjee R, Ikonomidis JS: Spatiotemporal expression and localization of matrix metalloproteinase-9 in a murine model of thoracic aortic aneurysm. J Vasc Surg 2006, 44:1314–1321
14. Junqueira LC, Bignolas G, Brentani RR: Picrosirius staining plus polarization microscopy, a specific method for collagen detection in tissue sections. Histochem J 1979, 11:447–455
15. Fitch RM, Rutledge JC, Wang YX, Powers AF, Tseng JL, Clary T, Rubanyi GM: Synergistic effect of angiotensin II and nitric oxide synthase inhibitor in increasing aortic stiffness in mice. Am J Physiol Heart Circ Physiol 2006, 290:H1190–H1198
16. Michel JB, Heudes D, Michel O, Poitevin P, Philippe M, Scalbert E, Corman B, Levy BI: Effect of chronic ANG I-converting enzyme inhibition on aging processes. II. Large arteries. Am J Physiol 1994, 267:R124–R135
17. Akishima Y, Akasaka Y, Ishikawa Y, Lijun Z, Kiguchi H, Ito K, Itabe H, Ishii T: Role of macrophage and smooth muscle cell apoptosis in association with oxidized low-density lipoprotein in the atherosclerotic development. Mod Pathol 2005, 18:365–373
18. Clarke MC, Figg N, Maguire JJ, Davenport AP, Goddard M, Littlewood TD, Bennett MR: Apoptosis of vascular smooth muscle cells induces features of plaque vulnerability in atherosclerosis. Nat Med 2006, 12:1075–1080
19. Marchand EL, Der Sarkissian S, Hamet P, deBlois D: Caspase-dependent cell death mediates the early phase of aortic hypertrophy regression in losartan-treated spontaneously hypertensive rats. Circ Res 2003, 92:777–784
20. Della Corte A, De Santo LS, Montagnani S, Quarto C, Romano G, Amarelli C, Scardone M, De Feo M, Cotrufo M, Caianiello G: Spatial patterns of matrix protein expression in dilated ascending aorta with aortic regurgitation: congenital bicuspid valve versus Marfan's syndrome. J Heart Valve Dis 2006, 15:20–27; discussion 27
21. Irizarry E, Newman KM, Gandhi RH, Nackman GB, Halpern V, Wishner S, Scholes JV, Tilson MD: Demonstration of interstitial collagenase in abdominal aortic aneurysm disease. J Surg Res 1993, 54:571–574
22. Raffetto JD, Khalil RA: Matrix metalloproteinases and their inhibitors in vascular remodeling and vascular disease. Biochem Pharmacol 2008, 75:346–359
23. Agozzino L, Sante P, Ferraraccio F, Accardo M, De Feo M, De Santo LS, Nappi G, Agozzino M, Esposito S: Ascending aorta dilatation in aortic valve disease: morphological analysis of medial changes. Heart Vessels 2006, 21:213–220
24. Cotrufo M, Della Corte A, De Santo LS, Quarto C, De Feo M, Romano G, Amarelli C, Scardone M, Di Meglio F, Guerra G, Scarano M, Vitale S, Castaldo C, Montagnani S: Different patterns of extracellular matrix protein expression in the convexity and the concavity of the dilated aorta with bicuspid aortic valve: preliminary results. J Thorac Cardiovasc Surg 2005, 130:504–511
25. de Figueiredo Borges L, Jaldin RG, Dias RR, Stolf NA, Michel JB, Gutierrez PS: Collagen is reduced and disrupted in human aneurysms and dissections of ascending aorta. Hum Pathol 2008, 39:437–443
26. Barbour JR, Stroud RE, Lowry AS, Clark LL, Leone AM, Jones JA, Spinale FG, Ikonomidis JS: Temporal disparity in the induction of matrix metalloproteinases and tissue inhibitors of metalloproteinases after thoracic aortic aneurysm formation. J Thorac Cardiovasc Surg 2006, 132:788–795
27. Brower GL, Gardner JD, Forman MF, Murray DB, Voloshenyuk T, Levick SP, Janicki JS: The relationship between myocardial extracellular matrix remodeling and ventricular function. Eur J Cardiothorac Surg 2006, 30:604–610
28. Spinale FG: Myocardial matrix remodeling and the matrix metalloproteinases: influence on cardiac form and function. Physiol Rev 2007, 87:1285–1342
29. Basalyga DM, Simionescu DT, Xiong W, Baxter BT, Starcher BC, Vyavahare NR: Elastin degradation and calcification in an abdominal aorta injury model: role of matrix metalloproteinases. Circulation 2004, 110:3480–3487
30. Kowalewski R, Sobolewski K, Malkowski A, Wolanska M, Gacko M: Evaluation of enzymes involved in proteoglycan degradation in the wall of abdominal aortic aneurysms. J Vasc Res 2006, 43:95–100
31. Springer TA: Monoclonal antibody analysis of complex biological systems. Combination of cell hybridization and immunoadsorbents in a novel cascade procedure and its application to the macrophage cell surface. J Biol Chem 1981, 256:3833–3839
32. Springer T, Galfre G, Secher DS, Milstein C: Mac-1: a macrophage differentiation antigen identified by monoclonal antibody. Eur J Immunol 1979, 9:301–306
33. Goldsmith EC, Hoffman A, Morales MO, Potts JD, Price RL, McFadden A, Rice M, Borg TK: Organization of fibroblasts in the heart. Dev Dyn 2004, 230:787–794
34. Osborn M, Weber K: Tumor diagnosis by intermediate filament typing: a novel tool for surgical pathology. Lab Invest 1983, 48:372–394
35. Rungger-Brandle E, Gabbiani G: The role of cytoskeletal and cytocontractile elements in pathologic processes. Am J Pathol 1983, 110:361–392
36. Skalli O, Schurch W, Seemayer T, Lagace R, Montandon D, Pittet B, Gabbiani G: Myofibroblasts from diverse pathologic settings are heterogeneous in their content of actin isoforms and intermediate filament proteins. Lab Invest 1989, 60:275–285

37. Babu GJ, Warshaw DM, Periasamy M: Smooth muscle myosin heavy chain isoforms and their role in muscle physiology. Microsc Res Tech 2000, 50:532–540
38. Frangogiannis NG, Michael LH, Entman ML: Myofibroblasts in reperfused myocardial infarcts express the embryonic form of smooth muscle myosin heavy chain (SMemb). Cardiovasc Res 2000, 48:89–100
39. Eyden B: The myofibroblast: phenotypic characterization as a prerequisite to understanding its functions in translational medicine. J Cell Mol Med 2008, 12:22–37
40. Gabbiani G: The biology of the myofibroblast. Kidney Int 1992, 41:530–532
41. Hinz B: Formation and function of the myofibroblast during tissue repair. J Invest Dermatol 2007, 127:526–537
42. Schurch W, Seemayer TA, Gabbiani G: The myofibroblast: a quarter century after its discovery. Am J Surg Pathol 1998, 22:141–147
43. Frangogiannis NG: The mechanistic basis of infarct healing. Antioxid Redox Signal 2006, 8:1907–1939
44. Sakata N, Nabeshima K, Iwasaki H, Tashiro T, Uesugi N, Nakashima O, Ito H, Kawanami T, Furuya K, Kojima M: Possible involvement of myofibroblast in the development of inflammatory aortic aneurysm. Pathol Res Pract 2007, 203:21–29
45. Shi Y, O'Brien JE, Jr., Fard A, Zalewski A: Transforming growth factor-β1 expression and myofibroblast formation during arterial repair. Arterioscler Thromb Vasc Biol 1996, 16:1298–1305
46. Vaughan MB, Howard EW, Tomasek JJ: Transforming growth factor-β1 promotes the morphological and functional differentiation of the myofibroblast. Exp Cell Res 2000, 257:180–189
47. Jones JA, Barbour JR, Stroud RE, Bouges S, Stephens SL, Spinale FG, Ikonomidis JS: Altered transforming growth factor-β signaling in a murine model of thoracic aortic aneurysm. J Vasc Res 2008, 45:457–468
48. Coucke PJ, Willaert A, Wessels MW, Callewaert B, Zoppi N, De Backer J, Fox JE, Mancini GM, Kambouris M, Gardella R, Facchetti F, Willems PJ, Forsyth R, Dietz HC, Barlati S, Colombi M, Loeys B, De Paepe A: Mutations in the facilitative glucose transporter GLUT10 alter angiogenesis and cause arterial tortuosity syndrome. Nat Genet 2006, 38:452–457
49. Kresse H, Schonherr E: Proteoglycans of the extracellular matrix and growth control. J Cell Physiol 2001, 189:266–274